

The impacts from SrS:Cu⁺,Na and LaOF:Eu³⁺ phosphors on color and luminous performances at 5600 K–8000 K WLEDs

Ha Thanh Tung¹, Huu Phuc Dang²

¹Faculty of Basic Sciences, Vinh Long University of Technology Education, Vinh Long Province, Vietnam

²Faculty of Fundamental Science, Industrial University of Ho Chi Minh City, Ho Chi Minh City, Vietnam

Article Info

Article history:

Received Sep 10, 2022

Revised Jan 10, 2023

Accepted Jan 14, 2023

Keywords:

Color rendering indices

Dual-layer remote phosphor

Lumen efficiency

Mie-scattering hypothesis

Remote-phosphor layer

Triple-layer remote phosphor

ABSTRACT

In terms of lumen performance, the remote phosphor structure can yield better results than the conformal phosphor and in-cup phosphor packages. The application of such a package in LEDs might make the manipulation of the device's chromatic performance challenging. Two remote phosphor packages are available for raising chromatic performance: one-layer and triple-layer phosphor adjustments. Using software simulation and phosphors created through specific procedures, our study was carried out to select the best adjustment that provides the best results in white LEDs (WLEDs) implemented with many chips: color rendering index (CRI), color quality scale (CQS), lumen output (LO), along with chromatic uniformity. We utilized the WLEDs at five temperatures of color between 5,600 K and 8,500 K. From the outcome, we can consider the three-layer phosphor package to have greater CRI, CQS, and lumen efficiency (LE). Notably, CQS and LE receive a roughly 30% boost compared to singular-layer package. The package can also reduce the chromatic deviation by roughly 30% to 50%, and therefore, grants a boost in chromatic homogeneity. To authenticate these outcomes, the dispersion attribute underwent examination in the layers of phosphor based on Mie-dispersion hypothesis. The outcome may prove useful for creating WLED devices with greater standards.

This is an open access article under the [CC BY-SA](https://creativecommons.org/licenses/by-sa/4.0/) license.



Corresponding Author:

Huu Phuc Dang

Faculty of Fundamental Science, Industrial University of Ho Chi Minh City

No. 12 Nguyen Van Bao Street, Ho Chi Minh City, Vietnam

Email: danghuuphuc@iuh.edu.vn

1. INTRODUCTION

The diodes that generate white light (WLEDs) possess various strengths, such as significant performance, little power requirement, great longevity, harmless to the environment, and therefore, have the potential to become the new optical sources and a substitute for standard incandescent lamps as well as fluorescent ones in many fields such as universal illumination, motor vehicle illumination and backlight [1]-[3]. The creation of WLEDs involves the most widely used means of integrating the GaN LED chip featuring the yellow-emitting Y₃Al₅O₁₂:Ce³⁺ (YAG) phosphor. The flaw of the WLEDs created is the inferior color rendering indices (CRI, Ra over 80) caused by the red light's shortage in the yellow phosphor's emission spectrum [4]. When increasing the red light and chromatic performance is the goal, we need to blend the red phosphors with the yellow phosphor. Then the WLEDs integrated with such phosphors can become suitable for commercial application [5], [6]. But a problem remains: due to the lack of the ability in our eyes to process the deep red element in red emission at the wavelength over 650 nm, the lumen efficiency (LE) in these WLEDs is not significant [7]. Colloidal quantum dots (QDs), in the recent times, have been recognized as a potential substitute for standard phosphor substances to transmute WLEDs' chromatic substances, thanks to their various

attribute of thin emission spectrum, broad absorption spectrum, as well as attributes of standard inorganic phosphor gained from the handling of solution [8]-[10]. There is a number of QDs versions, such as CdSe, InP, CuInS₂, C, CH₃NH₃PbBr₃, etc., that are gaining more and more recognition. The commercial CdSe is the best choice of all mentioned versions. Such QDs are classified as a semiconductor in the group II-VI, which possess a fairly thin entire width at half of the peak value (abbreviated as FWHM) (from 20 to 30 nm) along with outstanding quantum efficacy (over 95%). In addition, we can adjust the size of granules to let the QDs envelop all the observable zones. Thanks to the attributes mentioned, the CdSe QDs have great potential to be used in LEDs facets such as backlight presentation and universal illumination [11]. The QDs used in the earliest WLED model with an on-chip design based on QDs were, in fact, the CdSe QDs [9]. It should be noted that these QDs see little practical use as it consists of the Cd component, which is harmful to our health. QDs that do not contain the Cd component are eventually created to avoid health-related flaws, such as InP, CuInS₂, and carbon QDs. The InP and CuInS₂ QDs, however, provide smaller efficiency and broader full width at half maximum (FWHM) than the CdSe QDs [12]. The carbon QDs, on the other hand, struggles in the task of generating emission with long wavelengths (red emission, for example) [13]. In recent times, the perovskite QDs such as CH₃NH₃PbBr₃ and CsPbBr₃ are becoming more prominent optical substances thanks to their significant performance, and excellent chromatic genuineness, especially green [14]. The perovskite QDs provide thinner FWHM than the CdSe QDs. We can also adjust compositions to adapt them to various emission wavelengths. It is worth noting that it can be an issue to stabilize the QDs in the air environment, notably those that have red or blue color [15]. In general, we can consider the red CdSe QD optimal in boosting CRI value in standard WLED devices.

The remote phosphor package that divides the QDs sheets and the chip of LED is often applied to the majority of WLEDs integrated with QDs because of its considerable performance and better consistency of photon and heat [16]. However, if we combine phosphor and QDs to form a layer used for optical conversion, it will result in an inferior efficiency of light and heat in the WLED device, which is caused by the reabsorption occurring between phosphor and QDs as well as an insignificant performance of energy transmission between excitation light and substances used for optical conversion. These flaws of mixed-type WLED devices can be resolved by using a package with layers in an upright position to divide the phosphor and QDs layers in an upright direction, which is supposed to boost the efficiency of light and heat in WLED devices [17], [18]. The references support the placement of the phosphor layer close to the chip of LED, as it can result in a superior phosphor quantum compared to the QDs and the layer placed next the LED has a significant influence on chromatic transmutation. From the references, we can assume that the QDs-on-phosphor setting yielded superior LE, CRI values as well as inferior temperature of the WLED compared to the mixed version and phosphor-on-QDs version. The QDs-on-phosphor version, as a result, became a desirable means of achieving superior efficiency of light and heat. But still, the package mentioned cannot eliminate the repeating absorption since the red QDs can assimilate the phosphor's green or yellow illumination when it bypasses the layer of QDs. Also, the performance of energy transmission between the blue light and the layer of phosphor or QD will change over the surface of the layer due to the LED's Lambertian dispersion of intensity, which achieves the highest value in the central position and a fairly small value on the rim. The package placed over the lying-down surface has not been examined so far. This study recommends using a package with layers placed horizontally for the QDs phosphor nano-compound to remedy the issues of reabsorption and insignificant energy transmission at the same time. The nano-compound mentioned is shown to be able to substantially boost the efficiency of light and heat in WLEDs. For a comprehensive evaluation, we created three versions of WLEDs, which are QDs-phosphor blended, QDs-exterior, and QDs-interior versions, then determined their attributes of light and heat at many QDs-phosphor concentrations.

2. METHOD

2.1. Creating LaOF:Eu³⁺

Table 1 details the chemical composition of red-emission LaOF:Eu³⁺ phosphor. The preparation of LaOF:Eu³⁺ begins with slurring the ingredients in either water or methanol to create a mixture [19]. The mixture is then let dry within air and ground when dried. The mixture will be subject to certain heating stages. For the initial stage, the blend is burned at the temperature of 1,000 °C inside the capped quartz pipes accompanied by N₂ for an hour then pulverized afterward. In the next stage, the mixture is fired again with the same procedure but under the heat of 1,200 °C. The phosphor acquired has the red discharge, the discharge apex of 1.981 to 2.145 eV with the major line at 1.981 eV and excitation efficacy by UV of + (4.88 eV) and - (3.40 eV).

Table 1. Chemical constituents for red phosphor

Ingredient	Mole %	By weight (g)
La ₂ O ₃	61 (of La)	99.4
Eu ₂ O ₃	5 (of Eu)	8.8
LaF ₃	34	66.6

Table 2 presents the chemical ingredients essential for the preparation of green-emission SrS:Cu⁺,Na phosphor. The preparation of the phosphor SrS:Cu⁺,Na begins with dissolving the CuSO₄ along with NaHCO₃ in water, then the acquired solution is mixed with SrCO₃. Prepare a homogeneous slurry using either water or methanol, dry the blend, then mash it. Next, fire the blend within unclosed alumina boats with H₂S under 1200 °C within sixty minutes, then grind it. The mixture is to be stored in a well-closed container. The phosphor acquired has the green emission, 2.33 eV discharge apex, 0.31 eV emission width (FWHM), ++ (4.88 eV), ++ (3.40 eV) excitation efficiency by UV, high excitation efficacy by e-beam of ++ and non-exponential decay in the 10 μsec range along with prolonged phosphorescence [20].

Table 2. Chemical composition of green phosphor SrS:Cu⁺,Na

Ingredient	Mole %	By weight (g)
SrCO ₃	100	148
CuSO ₄ ·5 H ₂ O	0.1	0.250
NaHCO ₃	2	1.68

2.2. Simulation process

Figure 1 demonstrates illustration of the two WLED models simulated with the nine LED chips of WLED and two different remote-phosphor layer configurations. Every blue color chip at 453 nm the peak wavelength yields 1.16W. The singular-sheet distant phosphor formation (SL) integrated into a yellow layer YAG:Ce³⁺ phosphor, which is placed the chips of LED can be seen in Figure 1(a). The three-sheet distant phosphor formation (TL) integrated into the green layer SrS:Cu⁺,Na phosphor placed in the middle of the red and yellow phosphor layers is displayed in Figure 1(b). The recreated phosphor will be YAG:Ce³⁺ having a base as aluminium nitride. The CCT levels for packages will be 6,600 K and 7,700 K for the sake of precision. The tests will be seen throughout an upright axis.

The default thickness of every phosphor layer is 0.08 mm. Furthermore, altering YAG:Ce³⁺ content in response to variations for the red or yellow phosphor content will be vital, allowing the sustainment of an average level of the correlated color temperatures (ACCTs). The content for yellow phosphor YAG:Ce³⁺ can change accordingly to every ACCT level of every remote phosphor package, leading to various dispersion attributes of the LEDs and subsequently various light attributes.

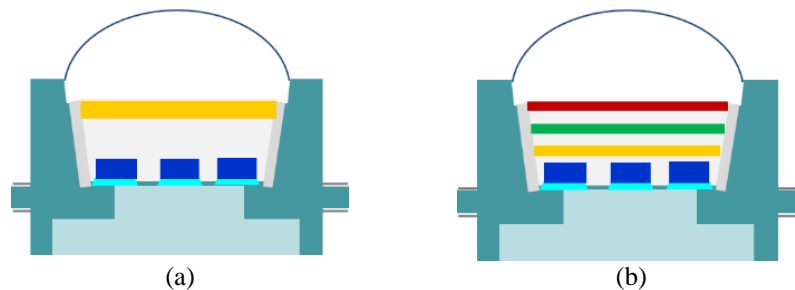


Figure 1. WLED's patterns involving multiple phosphor sheets: (a) single-sheet and (b) three-sheet

In Figure 2, regardless of ACCTs, the YAG:Ce³⁺ concentration reaches the biggest value in the SL package and the smallest value in the TL structure. If we evaluate all the packages at an identical ACCT level, the concentration of the yellow phosphor will increase when the 180°-reflection increases in occurrence, which will lead to a lower lumen value. Moreover, the significant concentration of the yellow phosphor can cause the disproportion between the three key colors that generate the white light (red, yellow, and green), lowering the WLEDs' optical performance. Thus, we must reduce the 180°-reflection phenomenon and maintain the chromatic consistency between the red, yellow, and green colors. We can also manipulate the color rendering index (CRI) via raising the red-light presence. In the case of the chromatic consistency and lumen, they can be manipulated via raising the green-light presence. With the prospect stated, the tri-sheet remote phosphor setting can become the superior option if the task is to manipulate optical attributes. To verify such a statement, we will showcase more crucial data on the emission spectrum in the remote phosphor packages in Figure 3. Judging the five ACCT levels, the SL package's emission spectrum scores the smallest intensity of the two packages, which indicates the smallest lumen in the package. On the other hand, the TL package has the greatest value of spectrum density in the wavelength range value between 380 and 780 nm.

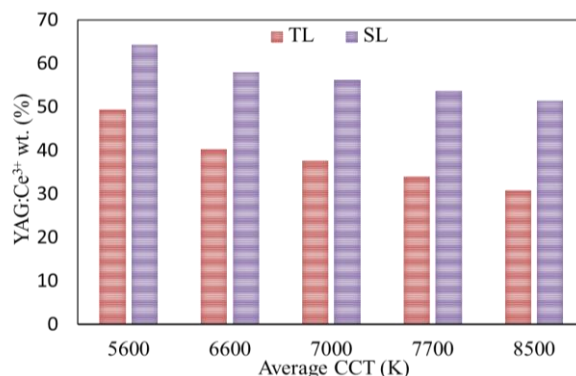


Figure 2. The YAG:Ce³⁺ content on distant phosphor configurations under disparate ACCT levels

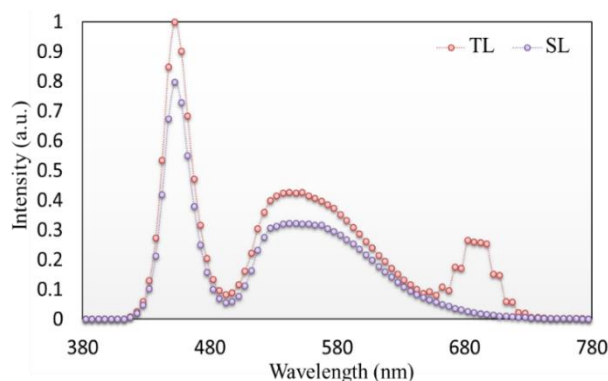


Figure 3. Emission spectra for phosphor configuration

3. RESULTS AND DISCUSSION

Figure 4 displays the color rendering indices values of the remote phosphor package. At every ACCT, the TL setting scores the best CRI. We can see that CRI correlates with ACCT, with CRI scoring the biggest value at the temperature of 8,500 K. Thanks to this outcome, the remote phosphor package can be useful for increasing the WLEDs' CRI value. The TL package is also useful for the task of manipulating the CRI at significant ACCT levels which exceed 7,000 K. When CRI results are compared, the TL package seems to have the second-highest value, which is also the smallest. The outcomes confirm that the TL package should be optimal for the large-scale fabrication for WLED devices having significant CRI. The CRI, however, would be simply among the many parameters used to determine chromatic performance in WLEDs. Many researchers have recently studied the color quality scale (CQS) parameter, being the combination of CRI, viewer's taste, along with chromatic coordinates. For combining three aspects, CQS has become the best parameter used to rate the chromatic performance, which is a considerable breakthrough.

Figure 5 showcases the CQS results for the phosphor settings. The TL setting gains the best CRI and therefore, has the best CQS. The SL package can generally benefit the lumen, but it cannot manage the chromatic performance without the extra green and red-light elements. The SL package may have a negative impact on chromatic performance, but its preparation procedure is easier and require fewer resources than the SL package, which can be very useful for manufacturing. Figure 5 verifies that the TL package should be chosen when the ultimate goal of the producers is chromatic performance. But if we improve the chromatic performance, will there be any disadvantage for the lumen? We will proceed to assess the lumen in the singular-sheet as well as dual-sheet packages. The upcoming section demonstrates the equations for the blue and yellow illumination (transmitted and converted respectively) in the structure of a two-layer phosphor, which could result in a remarkable improvement of the performance of the LED. The equations below present the blue and yellow light (transmitted and converted respectively) of a singular-sheet setting containing one phosphor sheet at 2h breadth [21]-[23].

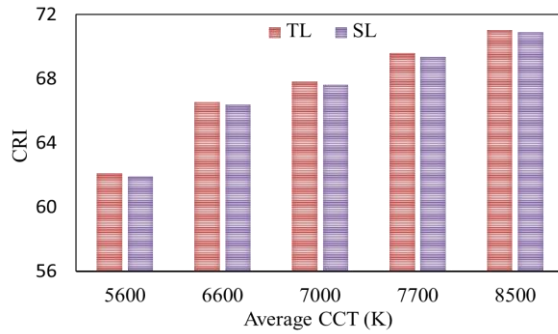


Figure 4. Color rendering indices for ACCT-corresponding phosphor setups

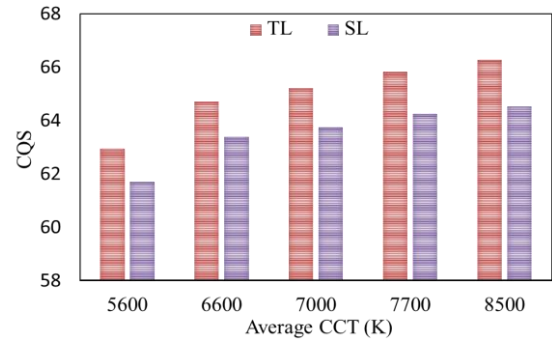


Figure 5. Color quality scale for ACCT-corresponding phosphor setups

$$PB_1 = PB_0 \times e^{-2\alpha_{B1}h} \quad (1)$$

$$PY_1 = \frac{1}{2} \frac{\beta_1 \times PB_0}{\alpha_{B1} - \alpha_{Y1}} (e^{-2\alpha_{Y1}h} - e^{-2\alpha_{B1}h}) \quad (2)$$

The following (3) and (4) exhibit the rays of a dual-sheet setting containing phosphor sheets at 2h breadth:

$$PB_2 = PB_0 \times e^{-2\alpha_{B2}h} \quad (3)$$

$$PY_2 = \frac{1}{2} \frac{\beta_2 \times PB_0}{\alpha_{B2} - \alpha_{Y2}} (e^{-2\alpha_{Y2}h} - e^{-2\alpha_{B2}h}) \quad (4)$$

For the (5), the h symbol indicates the width of every phosphor layer. The numbers 1 and 2 below the letters will stand for the singular-sheet and dual-sheet structures. β stands for the coefficient for the blue illumination transmutation into yellow. The reflection coefficient for the yellow ray would be signified via γ . The PB (blue illumination strength) as well as PY (yellow illumination strength) symbols, combined into PB_0 , stand for the ray strength from the LED in blue. α_B and α_Y stand for the insignificant power dissipation degree for said illumination throughout the propagation for the phosphor sheet. When compared to a singular-sheet setting, the dual-sheet setting greatly augments the light output for the LED device based on conversion phosphor:

$$\frac{(PB_2 + PY_2) - (PB_1 + PY_1)}{PB_1 + PY_1} > 0 \quad (5)$$

Our investigation uses the hypothesis of Mie-scattering to assess the phosphor particles' dispersion. Also, with the Mie theory [21]-[23], the dispersed cross-section C_{sca} in rounded granules will be assessed via a formula below. We utilize the law of Lambert-Beer [24], [25] for the task of gauging the energy for propagated illumination:

$$I = I_0 \exp(-\mu_{ext}L) \quad (6)$$

The I_0 symbol stands for the incident light energy, the L symbol stands for the width for the phosphor sheet (mm) with the μ_{ext} symbol standing for the extinction coefficient, assessed as: $\mu_{ext} = N_r \cdot C_{ext}$ where N_r signifies the particle density dispersion (mm^{-3}). C_{ext} (mm^2) is the phosphor granule absorption cross-section. With the (5), we can confirm that using additional phosphor layers can give a better lumen result compared to having just one layer, which is further validated by Figure 6 showing that the SL package possesses the worst lumen, regardless of ACCT level. On the contrary, the best lumen result belongs to the TL package. Judging the outcomes, the TL package can certainly yield the best chromatic performance. This indicates that it can limit the optical backscattering when the YAG:Ce^{3+} content diminishes. Also, compared to other layers, the yellow phosphor layer allows the LED chips' blue light to bypass it more effectively, indicating that the blue ray energy within the TL package is converted with great efficiency. As a result, the package obtains the greatest spectral density in the white light wavelength zone, which results in the best lumen.

The outcomes show that we can pick the TL package as a suitable option as it offers better light attributes for WLEDs, which are CQS and LE [24], [25]. But if chromatic performance is our main focus, we must take chromatic consistency into account. Many means are available for us to boost chromatic consistency. For example, utilizing the dispersing granules of SiO_2 , CaCO_3 , or conformal phosphor package. Such means may be able to boost the chromatic consistency, but as a result, we will acquire less lumen. When we take advantage of the green phosphor $\text{SrS}:\text{Cu}^+, \text{Na}$, and red phosphor $\text{LaOF}:\text{Eu}^{3+}$, we can improve the white light by increasing the dispersion and adding extra green and red-light elements to the WLEDs. The distant phosphor packages can also increase lumen efficiency as there is less back-scattering to the chip of LED. On the other hand, we still have to suitably modify the phosphor layer's concentration so that we can obtain the ideal energy propagated. The Lambert-Beer law utilized in (6) serves as a basis for such a statement. The chromatic deviation for every remote phosphor package is displayed in Figure 7. The chromatic consistency is inversely proportional to the chromatic deviation. We can notice that the lowest chromatic deviation belongs to the TL package. We can still manifest such an outcome, even though the dispersion in the LED happens prior to the appearance of the white light. When we add additional layers of phosphor, we can encourage dispersion, which will boost the chromatic consistency. On the other hand, the lumen will go down when we increase the dispersion. But the lower lumen is still a fair drawback when we consider the advantages of having less 180° reflection. In the end, the TL package can simultaneously yield the most ideal chromatic consistency and a reasonable lumen. On the other hand, at every ACCT level, the SL package produces the greatest chromatic deviation.

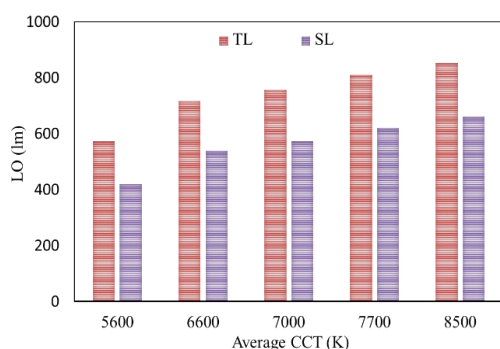


Figure 6. The phosphor compositions with the luminous output (LO) correspond to ACCTs

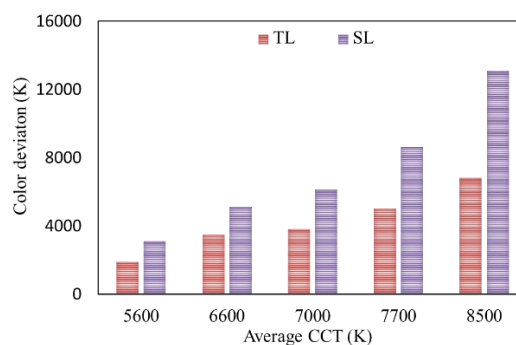


Figure 7. The phosphor compositions with correlated color temperature variation (D-CCT) correspond to ACCTs

4. CONCLUSION

This study examines the light efficacy in the SL and TL packages at five ACCT levels. Furthermore, for the simulation task, we made use of the green phosphor $\text{SrS}:\text{Cu}^+, \text{Na}$, and red phosphor $\text{LaOF}:\text{Eu}^{3+}$. The Mie-scattering hypothesis along with the law of Lambert-Beer were used to validate the outcomes. Introducing one $\text{SrS}:\text{Cu}^+, \text{Na}$ sheet for the purpose of increasing the green-ray appearance will increase the chromatic consistency and the lumen created. The chromatic performance is obviously decided by the equilibrium of the key chromas: red, green, along with yellow. The TL package has the ability to control such colors. Its lower occurrence of 180° -reflection also results in a rise in the lumen, which is verified by the most ideal lumen efficiency result of the TL package. The outcomes of our study will assist the producers in choosing the best package for their aims in order to improve their WLEDs.




REFERENCES

- [1] G. Tan, Y. Huang, M. C. Li, S. L. Lee, and S. T. Wu, "High dynamic range liquid crystal displays with a mini-LED backlight," *Optics Express*, vol. 26, no. 13, pp. 16572-16584, Jun. 2018, doi: 10.1364/OE.26.016572.
- [2] P. Zhu, H. Zhu, G. C. Adhikari, and S. Thapa, "Design of circadian white light-emitting diodes with tunable color temperature and nearly perfect color rendition," *OSA Continuum*, vol. 2, no. 8, pp. 2413-2427, Jul. 2019, doi: 10.1364/OSAC.2.002413.
- [3] L. Yang, Q. Zhang, F. Li, A. Xie, L. Mao, and J. Ma, "Thermally stable lead-free phosphor in glass enhancement performance of light emitting diodes application," *Applied Optics*, vol. 58, no. 15, pp. 4099-4104, May. 2019, doi: 10.1364/AO.58.004099.
- [4] Y. Tian *et al.*, "Study of composite $\text{Al}_2\text{O}_3\text{-Ce:Y}_3\text{Mg}_1.8\text{Al}_1.4\text{Si}_1.8\text{O}_{12}$ ceramic phosphors," *Optics Letters*, vol. 44, no. 19, pp. 4845-4848, Sep. 2019, doi: 10.1364/OL.44.004845.
- [5] P. Zhu, H. Zhu, G. C. Adhikari, and S. Thapa, "Spectral optimization of white light from hybrid metal halide perovskites," *OSA Continuum*, vol. 2, no. 6, pp. 1880-1888, May. 2019, doi: 10.1364/OSAC.2.001880.
- [6] C. Wu *et al.*, "Phosphor-converted laser-diode-based white lighting module with high luminous flux and color rendering index," *Optics Express*, vol. 28, no. 13, pp. 19085-19096, Jun. 2020, doi: 10.1364/OE.393310.




- [7] G. E. Romanova, V. I. Batshev, and A. S. Beliaeva, "Design of an optical illumination system for a tunable source with acousto-optical filtering," *Journal of Optical Technology*, vol. 88, no. 2, pp. 66-71, Feb. 2021, doi: 10.1364/JOT.88.000066.
- [8] L. V. Labunets, A. B. Borzov, and I. M. Akhmetov, "Regularized parametric model of the angular distribution of the brightness factor of a rough surface," *Journal of Optical Technology*, vol. 86, no. 10, pp. 618-626, Dec. 2019, doi: 10.1364/JOT.86.000618.
- [9] Y. Liang *et al.*, "Phosphor-in-glass (PIG) converter sintered by a fast Joule heating process for high-power laser-driven white lighting," *Optics Express*, vol. 29, no. 10, pp. 14218-14230, May. 2021, doi: 10.1364/OE.419633.
- [10] M. Quesada *et al.*, "All-glass, lenticular lens light guide plate by mask and etch," *Optical Materials Express*, vol. 9, no. 3, pp. 1180-1190, Feb. 2019, doi: 10.1364/OME.9.001180.
- [11] J. R. Beattie and F. W. L. Esmonde-White, "Exploration of principal component analysis: deriving principal component analysis visually using spectra," *Applied Spectroscopy*, vol. 75, no. 4, pp. 361-375, Jan. 2021, doi: 10.1177/0003702820987847.
- [12] B. Wang, D. S. Li, L. F. Shen, E. Y. B. Pun, and H. Lin, "Eu³⁺ doped high-brightness fluorophosphate laser-driven glass phosphors," *Optical Materials Express*, vol. 9, no. 4, pp. 1749-1762, Apr. 2019, doi: 10.1364/OME.9.001749.
- [13] Y. Wang *et al.*, "Tunable white light emission of an anti-ultraviolet rare-earth polysiloxane phosphors based on near UV chips," *Optics Express*, vol. 29, no. 6, pp. 8997-9011, Mar. 2021, doi: 10.1364/OE.410154.
- [14] H. Liu, Y. Shi, and T. Wang, "Design of a six-gas NDIR gas sensor using an integrated optical gas chamber," *Optics Express*, vol. 28, no. 8, pp. 11451-11462, Apr. 2020, doi: 10.1364/OE.388713.
- [15] T. Ya. Orudzhev, S. G. Abdullaeva, and R. B. Dzhabbarov, "Increasing the extraction efficiency of a light-emitting diode using a pyramid-like phosphor layer," *Journal of Optical Technology*, vol. 86, no. 10, pp. 671-676, Dec. 2019, doi: 10.1364/JOT.86.000671.
- [16] P. Kumar and N. K. Nishchal, "Enhanced exclusive-OR and quick response code-based image encryption through incoherent illumination," *Applied Optics*, vol. 58, no. 6, pp. 1408-1412, Feb. 2019, doi: 10.1364/AO.58.001408.
- [17] J. Li, Y. Tang, Z. Li, X. Ding, L. Rao, and B. Yu, "Investigation of stability and optical performance of quantum-dot-based LEDs with methyl-terminated-PDMS-based liquid-type packaging structure," *Optics Letters*, vol. 44, no. 1, pp. 90-93, Jan. 2019, doi: 10.1364/OL.44.000090.
- [18] Y. Li *et al.*, "395 nm GaN-based near-ultraviolet light-emitting diodes on Si substrates with a high wall-plug efficiency of 52.0% @ 350 mA," *Optics Express*, vol. 27, no. 5, pp. 7447-7457, Mar. 2019, doi: 10.1364/OE.27.007447.
- [19] M. J. Egan, A. M. Colón, S. M. Angel, and S. K. Sharma, "Suppressing the multiplex disadvantage in photon-noise limited interferometry using cross-dispersed spatial heterodyne spectrometry," *Applied Spectroscopy*, vol. 75, no. 2, pp. 208-215, Jul. 2020, doi: 10.1177/0003702820946739.
- [20] J. X. Yang, D. S. Li, G. Li, E. Y. B. Pun, and H. Lin, "Photon quantification in Ho³⁺/Yb³⁺ co-doped opto-thermal sensitive fluorotellurite glass phosphor," *Applied Optics*, vol. 59, no. 19, pp. 5752-5763, Jul. 2020, doi: 10.1364/AO.396393.
- [21] J. Hao, H. L. Ke, L. Jing, Q. Sun, and R. T. Sun, "Prediction of lifetime by lumen degradation and color shift for LED lamps, in a non-accelerated reliability test over 20,000 h," *Applied Optics*, vol. 58, no. 7, pp. 1855-1861, Mar. 2019, doi: 10.1364/AO.58.001855.
- [22] Y.-P. Chang *et al.*, "An advanced laser headlight module employing highly reliable glass phosphor," *Optics Express*, vol. 27, no. 3, pp. 1808-1815, Feb. 2019, doi: 10.1364/OE.27.001808.
- [23] Y. Yang *et al.*, "Low complexity OFDM VLC system enabled by spatial summing modulation," *Optics Express*, vol. 27, no. 21, pp. 30788-30795, Oct. 2019, doi: 10.1364/OE.27.030788.
- [24] I. Fujieda, Y. Tsutsumi, and S. Matsuda, "Spectral study on utilizing ambient light with luminescent materials for display applications," *Optics Express*, vol. 29, no. 5, pp. 6691-6702, Mar. 2021, doi: 10.1364/OE.418869.
- [25] N. C. A. Rashid *et al.*, "Spectrophotometer with enhanced sensitivity for uric acid detection," *Chinese Optics Letters*, vol. 17, no. 8, pp. 081701, Jul. 2019, doi: 10.3788/COL201917.081701.

BIOGRAPHIES OF AUTHORS



Ha Thanh Tung    received the PhD degree in physics from University of Science, Vietnam National University Ho Chi Minh City, Vietnam, he is working as a lecturer at the Faculty of Basic Sciences, Vinh Long University of Technology Education, Vietnam. His research interests focus on developing the patterned substrate with micro- and nano-scale to apply for physical and chemical devices such as solar cells, OLED, photoanode. He can be contacted at email: tunght@vlute.edu.vn.



Huu Phuc Dang    received a Physics Ph.D. degree from the University of Science, Ho Chi Minh City, in 2018. Currently, he is a lecturer at the Faculty of Fundamental Science, Industrial University of Ho Chi Minh City, Ho Chi Minh City, Vietnam. His research interests include simulation LEDs material, renewable energy. He can be contacted at email: danghuuphuc@iuh.edu.vn.